AIP | Applied Physics Letters

Rate-dependent stress evolution in nanostructured Si anodes upon lithiation

Zheng Jia and Wing Kam Liu

Citation: Applied Physics Letters **109**, 163903 (2016); doi: 10.1063/1.4964515
View online: http://dx.doi.org/10.1063/1.4964515
View Table of Contents: http://scitation.aip.org/content/aip/journal/apl/109/16?ver=pdfcov
Published by the AIP Publishing

Rate-dependent stress evolution in nanostructured Si anodes upon lithiation

Zheng Jia[a] and Wing Kam Liu[a]
Department of Mechanical Engineering, Northwestern University, Evanston, Illinois 60201, USA

(Received 13 May 2016; accepted 26 September 2016; published online 18 October 2016)

The development of stress and fracture in Si-based anodes for lithium-ion batteries is strongly affected by lithiation-induced plasticity. Recent experiments indicate that the nature of plasticity of lithiated silicon is rate-dependent. We establish a theoretical model to capture the viscoplastic mechanical behavior of Si anodes during two-phase lithiation. It is demonstrated that the lithiation-induced stress field is determined by the migration speed of the Li-$Li_{3.75}Si$ interface and the characteristic size of the Si anodes. If experimentally measured interface velocity data in Si nanoparticle are available, the mechanistic model can directly predict the rate-sensitive spatiotemporal stress profile, which is hardly measured in experiments. *Published by AIP Publishing.*
[http://dx.doi.org/10.1063/1.4964515]

Silicon is emerging as the most promising anode material for lithium-ion batteries, given its theoretical capacity as high as ten times as that of commercially available graphite-based anodes.[1] However, the large volume change (~300%) during lithium insertion/extraction may fracture the silicon anode and the solid-electrolyte interface (SEI),[2,3] resulting in irreversible capacity fading and poor cycle life.[4–6] Intensive research efforts have revealed that the development of stress and its associated fracture in Si anodes is strongly affected by lithiation-induced plasticity. Sethuraman *et al.* measured the stress evolution in Si thin-film electrodes during charging/discharging cycles and observed the plastic deformation of lithiated silicon with yielding stress measuring about 1.5 GPa.[7] The plastic deformation in lithiated silicon is postulated to be a consequence of the repeated breaking/forming of Si-Li bonds assisted by continuous Li insertion.[8,9] The plastic flow restricts the magnitude of lithiation-induced stress and thus the energy release rate for crack propagation (i.e., the crack driving force), preventing fracture of nano-sized (~100 nm) electrodes.[5]

Recently, experimental evidence has indicated that the nature of plasticity in lithiated silicon is rate-dependent. Constant-force creep tests conducted on fully lithiated c-$Li_{3.75}Si$ nanowires reveal a power-law creep behavior when the applied stress approaches the yield strength of the fully lithiated silicon, indicating a strong strain-rate dependence on stress.[10] Nanoindentation creep tests show that fully lithiated silicon creeps much more readily than does unlithiated amorphous silicon.[11] Besides fully lithiated silicon, partially lithiated silicon is also reported to exhibit time-dependent deformation behavior. *In-situ* stress measurements during electrochemical testing on amorphous Li_xSi thin films demonstrate that an increase in the rate of lithiation results in a corresponding increase in the stress, which follows a power-law relationship between the strain rate and the stress.[12] These studies are indicative of the viscoplastic behavior of lithiated-silicon: plastic flow in lithiated silicon is rate-sensitive. To facilitate the understanding of the dynamics of viscoplastic deformation in lithiated silicon, a mechanistic model that involves the rate-dependent behavior is highly desirable but still lacking.

Investigation of the concurrent lithiation and deformation in lithiated silicon via theoretical analysis[13,14] and chemo-mechanical modeling[6,15–17] has received enormous attention, largely due to the fact that lithiation-induced stress strongly influences the lithiation kinetics and mechanical failure of silicon anodes in lithium-ion batteries. Nevertheless, few efforts have been made to take viscoplasticity of lithiated silicon into account in existing theoretical models and chemo-mechanical simulations. To address the above concern, this work presents a mechanistic model considering two-phase lithiation and concurrent rate-dependent viscoplasticity. We study the two-phase lithiation process of a silicon nanoparticle, with an initial radius R_o at the reference state (Fig. 1(a)). Upon lithiation, a fully lithiated $Li_{3.75}Si$ shell is developed, as shown in Fig. 1(b). During this process, lithiated silicon expands in volume to accommodate the lithium insertion. Therefore, a material element characterized by the initial radius R in the reference state is deformed and moves to a position with radius r(t) in the current state after this material element is lithiated. In particular, the surface of the particle with an initial radius R_o is pushed out to be the current surface with a radius r_o. There exists a sharp interface between the unreacted pristine Si core and the $Li_{3.75}Si$ shell,

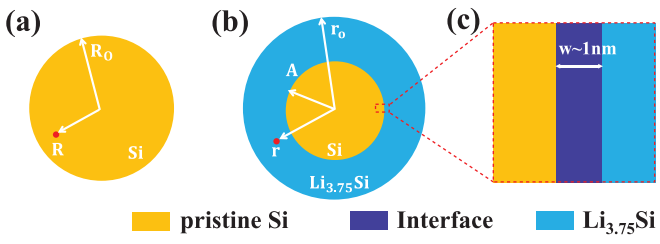

FIG. 1. (a) A pristine spherical silicon particle with an initial radius R_o is considered to be the reference state. A material point (labeled by the red dot) is at a radius R. (b) Upon lithiation, the outer surface is now at a radius r_o, and the material point labeled by R in the reference state moves to a location at a radius r. (c) The interface (dark blue) between the lithiated phase (cyan) and the pristine Si phase (yellow) is characterized by a radius of A(t) and a thickness of w (~1 nm).

[a]Electronic addresses: zheng.jia@northwestern.edu and w-liu@northwestern.edu

characterized by a radius of A (Fig. 1(b)). As the lithiation proceeds, the interface migrates towards the particle center, with A decreasing. Stress field arises and evolves in the Si nanoparticle in response to the migration of the interface. *In situ* atomic-scale TEM imaging has revealed that the interface has a thickness w which is about 1 nm (~3–4 atomic layers),[18] as illustrated in Fig. 1(c). Despite that w is trivial when compared to the nanoparticle size (~100 nm), we will demonstrate that the thickness w plays a role in determining the rate-dependent stress evolution while it can be ignored if lithiation-induced plasticity is assumed to be rate-independent.

Consider a shell of silicon between radii A and r in the current state, which results from the lithiation of a pristine silicon shell between radii A and R in the reference state. The current position r of a material element is determined by $\mathrm{r} = \left[\mathrm{A}^3 + \beta(\mathrm{R}^3 - \mathrm{A}^3)\right]^{\frac{1}{3}}$, here β is the volume expansion ratio defined by the volume of $Li_{3.75}Si$ over that of the pristine silicon. The hoop and radial stretches in the $Li_{3.75}Si$ shell are $\lambda_\theta = \frac{\mathrm{r}}{\mathrm{R}}$ and $\lambda_\mathrm{r} = \frac{\mathrm{R}^2}{\mathrm{r}^2}\beta$, respectively. The lithiation-induced deformation can be decomposed into three components: elastic, plastic, and volumetric deformation. During lithiation, the elastic strain is trivial compared with the plastic and volumetric strain and hence can be neglected. Therefore, the plastic stretches are given by $\lambda_\theta^\mathrm{p} = \frac{\mathrm{r}}{\mathrm{R}}\beta^{-\frac{1}{3}}$ and $\lambda_\mathrm{r}^\mathrm{p} = \frac{\mathrm{R}^2}{\mathrm{r}^2}\beta^{\frac{2}{3}}$. The plastic deformation gradient tensor $\mathbf{F}^\mathrm{p}$ can then be written as $\langle \frac{\mathrm{R}^2}{\mathrm{r}^2}\beta^{\frac{2}{3}},\ \frac{\mathrm{r}}{\mathrm{R}}\beta^{-\frac{1}{3}},\ \frac{\mathrm{r}}{\mathrm{R}}\beta^{-\frac{1}{3}}\rangle$.

Considering finite-strain viscoplasticity, the mechanical behavior of the $Li_{3.75}Si$ alloy is governed by

$$\mathbf{D}^\mathrm{p} = \frac{\partial \mathrm{G}(\sigma_\mathrm{eff})}{\partial \mathbf{S}}, \tag{1}$$

where $\mathbf{D}^\mathrm{p}$ is the plastic stretch rate tensor, $\mathbf{S}$ is the deviatoric stress tensor, σ_eff is the effective stress, and $\mathrm{G}(\sigma_\mathrm{eff})$ denotes the viscoplastic flow potential. In particular, we adopt a power-law flow potential of the form

$$\mathrm{G}(\sigma_\mathrm{eff}) = \frac{\sigma_\mathrm{Y}\dot{\mathrm{d}}}{\mathrm{m}+1}\left(\frac{\sigma_\mathrm{eff}}{\sigma_\mathrm{Y}} - 1\right)^{\mathrm{m}+1}, \tag{2}$$

where σ_Y, $\dot{\mathrm{d}}$, and m are material properties. σ_Y is the yield strength of the material, $\dot{\mathrm{d}}$ is the reciprocal of viscosity, and m is the stress exponent. Eq. (2) is only applicable when σ_eff exceeds σ_Y. The combination of Eqs. (1) and (2) gives the plastic stretch rate tensor $\mathbf{D}^\mathrm{p} = \mathrm{sgn}(\sigma_\mathrm{r} - \sigma_\theta)\dot{\mathrm{d}}\left(\frac{\sigma_\mathrm{eff}}{\sigma_\mathrm{Y}} - 1\right)^\mathrm{m}\langle 1, -\frac{1}{2}, -\frac{1}{2}\rangle$, where sgn(x) denotes the sign function. The plastic stretch rate tensor can also be derived by using the principal plastic deformation gradient tensor $\mathbf{F}^\mathrm{p}$ in an alternative way: $\mathbf{D}^\mathrm{p} = \dot{\mathbf{F}}^\mathrm{p}(\mathbf{F}^\mathrm{p})^{-1} = \langle \frac{\dot{\lambda}_\mathrm{r}^\mathrm{p}}{\lambda_\mathrm{r}^\mathrm{p}}, \frac{\dot{\lambda}_\theta^\mathrm{p}}{\lambda_\theta^\mathrm{p}}, \frac{\dot{\lambda}_\theta^\mathrm{p}}{\lambda_\theta^\mathrm{p}}\rangle = \frac{2(\beta-1)\mathrm{A}^2\dot{\mathrm{A}}}{\mathrm{r}^3}\langle 1, -\frac{1}{2}, -\frac{1}{2}\rangle$. Here, $\dot{\mathrm{A}}$ denotes the migration speed of the interface that can be quantitatively measured by *in situ* experiments. Comparing the two expressions of $\mathbf{D}^\mathrm{p}$ yields that $\frac{2(\beta-1)\mathrm{A}^2\dot{\mathrm{A}}}{\mathrm{r}^3} = \mathrm{sgn}(\sigma_\mathrm{r} - \sigma_\theta)\dot{\mathrm{d}}\left(\frac{\sigma_\mathrm{eff}}{\sigma_\mathrm{Y}} - 1\right)^\mathrm{m}$. Considering that the interface migrates towards the particle center ($\dot{\mathrm{A}} < 0$) during lithiation and $\beta = 4$ for fully lithiated silicon, we obtain

$$\sigma_\mathrm{r} - \sigma_\theta = -\left(\frac{\left[2(\beta-1)\mathrm{A}^2|\dot{\mathrm{A}}|\right]^\mathrm{n}}{\dot{\mathrm{d}}^\mathrm{n}\mathrm{r}^{3\mathrm{n}}} + 1\right)\sigma_\mathrm{Y}, \tag{3}$$

where n is the reciprocal of m. The force equilibrium on a material element requires that $\frac{\partial \sigma_\mathrm{r}}{\partial \mathrm{r}} = 2\frac{\sigma_\theta - \sigma_\mathrm{r}}{\mathrm{r}}$. Using Eq. (3) and integrating the equilibrium equation with traction-free boundary condition at $\mathrm{r} = \mathrm{r_o}$, we obtain the stress distribution in the $Li_{3.75}Si$ shell ($\mathrm{A} < r \le \mathrm{r_o}$)

$$\sigma_\mathrm{r} = \frac{2}{3\mathrm{n}}\left[2(\beta-1)\left(\frac{\mathrm{A}}{\mathrm{r_o}}\right)^2\frac{|\dot{\mathrm{A}}|}{\dot{\mathrm{d}}\mathrm{r_o}}\right]^\mathrm{n}\left[1 - \left(\frac{\mathrm{r_o}}{\mathrm{r}}\right)^{3\mathrm{n}}\right]\sigma_\mathrm{Y} + 2\log\left(\frac{\mathrm{r}}{\mathrm{r_o}}\right)\sigma_Y, \tag{4}$$

$$\sigma_\theta = \left[2(\beta-1)\left(\frac{\mathrm{A}}{\mathrm{r_o}}\right)^2\frac{|\dot{\mathrm{A}}|}{\dot{\mathrm{d}}\mathrm{r_o}}\right]^\mathrm{n}\left[\frac{2}{3\mathrm{n}} + \left(1 - \frac{2}{3\mathrm{n}}\right)\left(\frac{\mathrm{r_o}}{\mathrm{r}}\right)^{3\mathrm{n}}\right]\sigma_\mathrm{Y} + 2\log\left(\frac{\mathrm{r}}{\mathrm{r_o}}\right)\sigma_\mathrm{Y} + \sigma_\mathrm{Y}. \tag{5}$$

Eqs. (4) and (5) indicate that the rate-dependent lithiation-induced stress at a given position $\frac{\mathrm{r}}{\mathrm{r_o}}$ in the fully lithiated shell is determined by two dimensionless groups, i.e., the normalized interface position $\frac{\mathrm{A}}{\mathrm{r_o}}$ and the normalized interface migration velocity $\frac{|\dot{\mathrm{A}}|}{\dot{\mathrm{d}}\mathrm{r_o}}$. It demonstrates that the interface migration velocity $|\dot{\mathrm{A}}|$ affects the viscoplastic mechanical response of $Li_{3.75}Si$ alloy. On the contrary, if the plastic deformation of lithiated silicon is taken to be rate-independent as in previous studies,[13] the lithiation-induced stress and deformation in a silicon nanoparticle are determined merely by the interface position $\frac{\mathrm{A}}{\mathrm{r_o}}$, regardless of the interface speed.

For a material element on the interface, deformation along hoop directions is strongly constrained by the inner stiff unlithiated silicon core. As a result, stretch components can be written as $\lambda_\mathrm{r} = \beta$ and $\lambda_\theta = 1$. The associated plastic principal stretches are $\lambda_\mathrm{r}^\mathrm{p} = \beta^{2/3}$ and $\lambda_\theta^\mathrm{p} = \beta^{-\frac{1}{3}}$. To uncover the stress generation mechanism on the interface, we need to consider how the interface is lithiated. As noted above, although the interface is mathematically considered to be a line in the continuum-scale mechanistic model (Fig. 1(b)), it is a known fact that the interface thickness w is ~1 nm.[18] At the 1 nm-thick interface, lithium atoms gradually accumulate and react with silicon, forming a partially lithiated phase Li_xSi ($0 \le \mathrm{x} \le 3.75$). The lithium concentration at the interface can be equivalently characterized by x, i.e., the number of Li atoms hosted by one Si atom. The value of x increases as lithiation of interface advances and eventually reaches 3.75. The associated volume expansion ratio β ramps from 1 (pristine state, $\mathrm{x} = 0$) to 4 (fully lithiated state, $\mathrm{x} = 3.75$) as the lithium concentration accumulates at the interface. Therefore, in contrast to the deformation of the fully lithiated phase driven by the inward movement of the interface, the deformation of an interface at a given radius A is merely evolved by the change of local Li concentration, or equivalently the change of β at the interface. To this end, the plastic stretch rate tensor $\mathbf{D}^\mathrm{p}$ can be obtained as $\mathbf{D}^\mathrm{p} = \dot{\mathbf{F}}^\mathrm{p}(\mathbf{F}^\mathrm{p})^{-1} = \frac{2}{3}\frac{\dot{\beta}}{\beta}\langle 1, -\frac{1}{2}, -\frac{1}{2}\rangle$. Comparing the calculated $\mathbf{D}^\mathrm{p}$ with that obtained from Eqs. (1) and (2)

gives that $\frac{2}{3}\frac{\dot{\beta}}{\beta} = \mathrm{sgn}(\sigma_r - \sigma_\theta)\dot{d}\left(\frac{\sigma_{eff}}{\sigma_f} - 1\right)^m$. Here, we assume the changing rate of β, i.e., $\dot{\beta}$, is a constant within the interface of thickness w. Thus, $\dot{\beta}$ can be related to the migration velocity $|\dot{A}|$ of the interface (see the supplementary material for details)

$$|\dot{A}| = w \Big/ \left(\frac{\beta - 1}{\dot{\beta}}\right) = w \Big/ \left(\frac{3}{4}\frac{\beta}{\dot{\beta}}\right). \tag{6}$$

With Eq. (6), we link the stress state at the interface to the interface migration speed: $\frac{1}{2}\frac{|\dot{A}|}{w} = \mathrm{sgn}(\sigma_r - \sigma_\theta)\dot{d}\left(\frac{\sigma_{eff}}{\sigma_f} - 1\right)^m$. It indicates that $\sigma_r - \sigma_\theta > 0$. Reorganizing the equation yields that at the interface

$$\sigma_r - \sigma_\theta = \left[\left(\frac{1}{2}\frac{|\dot{A}|}{\dot{d}w}\right)^n + 1\right]\sigma_Y. \tag{7}$$

Radial stress σ_r is continuous across the interface; therefore, at the interface ($r = A$)

$$\frac{\sigma_r}{\sigma_Y} = \frac{2}{3n}\left[2(\beta - 1)\left(\frac{A}{r_o}\right)^2\frac{|\dot{A}|}{\dot{d}r_o}\right]^n\left[1 - \left(\frac{r_o}{A}\right)^{3n}\right] + 2\log\left(\frac{A}{r_o}\right). \tag{8}$$

A combination of Eqs. (7) and (8) determines the hoop stress on the interface

$$\frac{\sigma_\theta}{\sigma_Y} = \frac{2}{3n}\left[2(\beta - 1)\left(\frac{A}{r_o}\right)^2\frac{|\dot{A}|}{\dot{d}r_o}\right]^n\left[1 - \left(\frac{r_o}{A}\right)^{3n}\right] + 2\log\left(\frac{A}{r_o}\right) - \left(\frac{1}{2}\frac{|\dot{A}|}{\dot{d}w}\right)^n - 1. \tag{9}$$

The unlithiated silicon core ($0 \le r < A$) is in a state of hydrostatic compression, which is set by Eq. (8)

$$\frac{\sigma_r}{\sigma_Y} = \frac{\sigma_\theta}{\sigma_Y} = \frac{2}{3n}\left[2(\beta - 1)\left(\frac{A}{r_o}\right)^2\frac{|\dot{A}|}{\dot{d}r_o}\right]^n\left[1 - \left(\frac{r_o}{A}\right)^{3n}\right] + 2\log\left(\frac{A}{r_o}\right). \tag{10}$$

Eqs. (4)–(5) and (8)–(10) fully define the rate-sensitive lithiation-induced stress fields in the Si anodes. The strain rate effects are reflected by the contribution of interface migration speed $|\dot{A}|$. For quasi-static lithiation process, setting $|\dot{A}| = 0$ recovers the results of rate-independent plasticity model.[13] Moreover, based on the stress field equations, some key dimensionless groups/parameters governing the stress evolution can be determined: in the deformed state, the lithiation-induced stress field in the Si particle is governed by three dimensionless groups: $\frac{A}{r_o}$, $\frac{|\dot{A}|}{\dot{d}r_o}$, and $\frac{|\dot{A}|}{\dot{d}w}$. Equivalently, in the reference state, the stress field is dictated by $\frac{A}{R_o}$, $\frac{|\dot{A}|}{\dot{d}R_o}$, and $\frac{|\dot{A}|}{\dot{d}w}$. These dimensionless groups indicate that the interface migration velocity $|\dot{A}|$, the size of the Si nanoparticle R_o, and even the thickness of the interface w affect the stress development when the viscoplastic behavior of $Li_{3.75}Si$ phase is considered.

Fig. 2 plots the lithiation-induced stress field in the reference state when the reaction front is at $\frac{A}{R_o} = 0.8$ with various values of $\frac{|\dot{A}|}{\dot{d}R_o}$ (note that $\frac{|\dot{A}|}{\dot{d}w}$ is known once $\frac{|\dot{A}|}{\dot{d}R_o}$ is given). To make the plot, we adopt the following values for the power-law flow potential: $\dot{d} = 0.002/s$,[12] $n = 0.25$ (i.e., $m = 4$).[12] The interface thickness is set to be $w = 1\,nm$.[18] It is worth noting that in experiments the interface usually slows as it progresses into the Si particles, featuring a changing interface migration speed $|\dot{A}|$.[19] However, to focus on

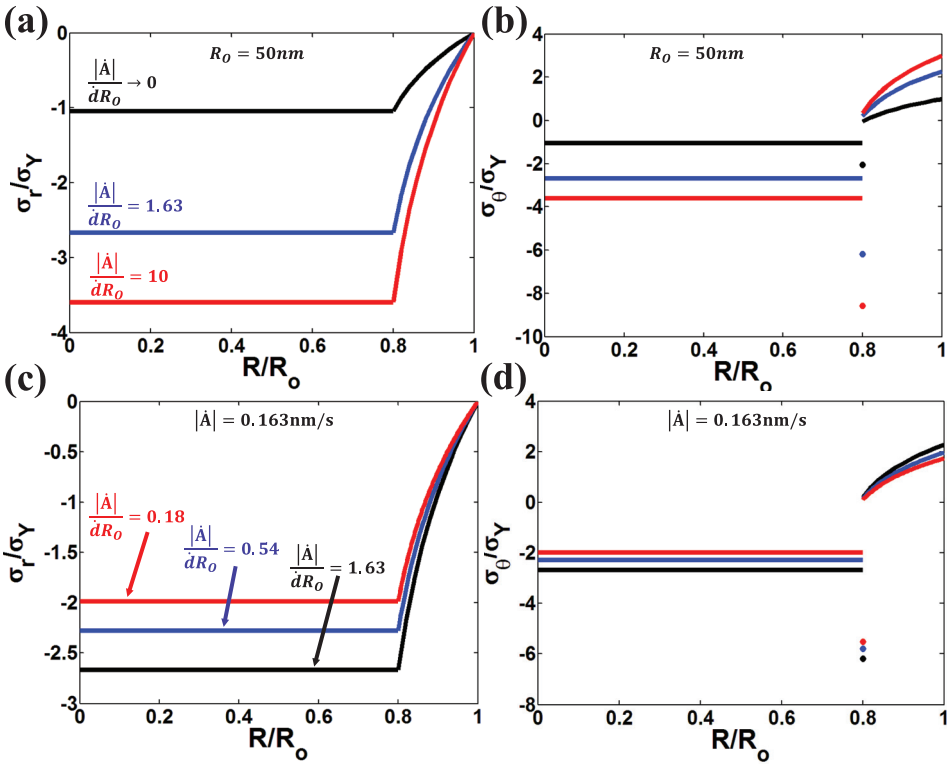

FIG. 2. Stress field in a spherical particle when the reaction front is at A/b = 0.8 with various values of $\frac{|\dot{A}|}{\dot{d}R_o}$. In a particle with given initial radius of 50 nm, (a) radial stress and (b) hoop stress rise in magnitude with increasing interface speed or charging rates. With a fixed interface velocity of 0.163 nm/s, (c) radial stress and (d) hoop stress rise in magnitude with decreasing particle size.

the influence of the interface speed on the stress evolution, without losing generality, in this work, we take $|\dot{A}|$ during lithiation as a constant. Figs. 2(a) and 2(b) plot the radial stress σ_r and the hoop stress σ_θ, respectively, in a Si particle with the given initial radius of 50 nm. Three representative values of $|\dot{A}|$ are chosen: (1) $|\dot{A}| = 1\,\text{nm/s}$ ($\frac{|\dot{A}|}{dR_o} = 10$), which is approximately the average of the experimentally recorded interface speed in Si anodes.[19] (2) $|\dot{A}| = 0.163\,\text{nm/s}$ ($\frac{|\dot{A}|}{dR_o} = 1.63$), the theoretical interface velocity along $\langle 110\rangle$ direction in crystalline silicon in the absence of stress and electrical potential. (3) $|\dot{A}| \to 0\,\text{nm/s}$ ($\frac{|\dot{A}|}{dR_o} = 0$), representing a quasi-static lithiation process. Comparing stress fields with different interface velocities concludes that faster charging, i.e., larger $|\dot{A}|$, results in higher stress in a given silicon particle—the Si particle undergoes increased compressive stress in the unlithiated core and increased tensile stress near the surface. In other words, Si anodes under a quasi-static lithiation process (black curves in Figs. 2(a) and 2(b)) undergo the lowest stress magnitude. To investigate the influence of particle size on stress development, Figs. 2(c) and 2(d) plot the radial stress σ_r and the hoop stress σ_θ, respectively, given a fixed interface velocity of $|\dot{A}| = 0.163\,\text{nm/s}$. Si particles with initial radii R_o of 50 nm, 150 nm, and 450 nm are considered. The corresponding dimensionless group $\frac{|\dot{A}|}{dR_o}$ equals to 1.63, 0.54, and 0.18, respectively. It is evident that larger particles experience less stress.

In situ TEM imaging has evidenced that silicon particles may undergo surface cracking during electrochemical lithiation.[5] The formation of cracks near the surface is closely related to the tensile hoop stress level near the particle surface. Fig. 3 plots hoop stress σ_θ at the surface layer of the Si particle as a function of the interface position A/R_o with various values of $\frac{|\dot{A}|}{dR_o}$. As shown in Fig. 3(a), in a Si particle with an initial radius of 50 nm, quasi-static lithiation process ($\frac{|\dot{A}|}{dR_o} \to 0\,\text{nm/s}$) leads to a constant hoop stress over time, i.e., $\sigma_\theta(R_o) = \sigma_Y$, independent on the interface position, which is in agreement with the prediction by rate-independent plasticity model for lithiated silicon.[13,20] The most salient feature of Fig. 3(a) is that faster migration, i.e., larger $\frac{|\dot{A}|}{dR_o}$, leads to higher hoop stress at the particle surface. This provides a direct physical appreciation of the experimentally observed charging-rate-dependent fracture of Si anodes.[21] It is also noted that $\sigma_\theta(R_o)$ decreases as the interface progresses toward the center of the particle. This is due to the fact that in Eq. (5) the dimensionless group $\frac{|\dot{A}|}{dr_o}$ decreases as the interface migrates away from the surface, indicating that the influence of the interface speed decreases as the lithiation proceeds. Fig. 3(b) shows the results of hoop stress evolution at the particle surface with a given interface migration speed $|\dot{A}| = 0.163\,\text{nm/s}$. As expected, larger particle undergoes smaller tensile hoop stress at the surface. The results from our model are predictive but need to be validated by high-fidelity experiments. An experimental technique using micro-Raman spectroscopy has been recently developed to directly measure lithiation-induced stress in nano-sized silicon particle.[22] It is expected that in the future such technique can be used to measure stress development in Si nanoparticles under various charging rates and validate our simulated results.

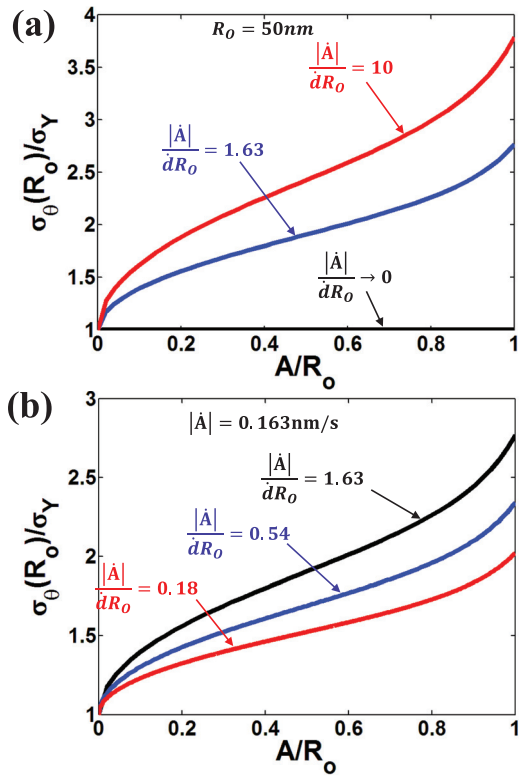

FIG. 3. Hoop stress at the particle surface as a function of interface position with various values of $\frac{|\dot{A}|}{dR_o}$. (a) Stress evolution in a given particle. (b) Stress evolution at a given interface velocity.

In this study, as noted above, the interface migration speed $|\dot{A}|$ is set to be a constant during lithiation to elucidate its influence on the stress development. It is worth mentioning that the formulated theory is also applicable to changing migration speed observed in experiments.[19] To predict the rate-sensitive stress field in a silicon nanoparticle under lithiation, experimentally measured interface speed history (e.g., speed vs. time) can be directly plugged into Eqs. (4)–(5) and (8)–(10) to calculate the evolution of the stress field. The mechanistic model presented in this work offers a powerful theoretical tool to capture the rate-sensitive stress development of Si anodes in lithium-ion batteries, which is hardly measured in experiments. Moreover, it is necessary to emphasize that the results reported in this work are only applicable to phase-changing material (e.g., crystalline silicon during lithiation) in which lithiation proceeds by the movement of a lithiation front which separates a pristine unreacted phase and a fully reacted phase. Lithiation of materials with other lithiation mechanisms requires further study and is beyond the scope of this paper.

In conclusion, we formulated a theoretical mechanistic model considering the viscoplastic mechanical behavior of lithiated silicon. It is shown that the viscoplasticity-regulated stress field is fully determined by three key dimensionless groups: the normalized interface position $\frac{A}{R_o}$, the normalized interface speed with respect to particle size $\frac{|\dot{A}|}{dR_o}$, and the normalized interface speed with respect to interface thickness

$\frac{|\dot{A}|}{dw}$. We demonstrate that larger values of $\frac{|\dot{A}|}{dR_o}$ results in larger stress in the anode, indicating that higher charging rates (i.e., higher interface speed) result in higher stress level, which is well in line with experimental observations.[11,12,21] In other words, we demonstrate that lithiation-induced stress is mainly affected by the migration speed of the Li-$Li_{3.75}Si$ interface and the characteristic size of the Si anodes. For quasi-static lithiation process, our model can readily reproduce the results of existing models considering rate-independent plasticity.[13,20] Moreover, this work provides a powerful theoretical tool to directly predict the rate-dependent stress profile in Si nanoparticle during lithiation by using experimentally recorded interface velocity data. Further experimental studies are expected to validate our mechanistic model.

See supplementary material for details of the interface model.

The authors would like to gratefully acknowledge the support for this work provided by the Center for Hierarchical Materials Design (CHiMaD) at Northwestern University under Grant No. 70NANB14H012.

[1]J. Li and J. R. Dahn, J. Electrochem. Soc. **154**, A156 (2007).
[2]K. Zhao, M. Pharr, L. Hartle, J. J. Vlassak, and Z. Suo, J. Power Sources **218**, 6 (2012).
[3]T. Zhu, Chin. Phys. B **25**, 014601 (2016).
[4]C. K. Chan, H. Peng, G. Liu, K. McIlwrath, X. F. Zhang, R. A. Huggins, and Y. Cui, Nat. Nanotechnol. **3**, 31 (2008).
[5]X. H. Liu, L. Zhong, S. Huang, S. X. Mao, T. Zhu, and J. Y. Huang, ACS Nano **6**, 1522 (2012).
[6]X. H. Liu, H. Zheng, L. Zhong, S. Huan, K. Karki, L. Q. Zhang, Y. Liu, A. Kushima, W. T. Liang, J. W. Wang, J.-H. Cho, E. Epstein, S. A. Dayeh, S. T. Picraux, T. Zhu, J. Li, J. P. Sullivan, J. Cumings, C. Wang, S. X. Mao, Z. Z. Ye, S. Zhang, and J. Y. Huang, Nano Lett. **11**, 3312 (2011).
[7]V. A. Sethuraman, M. J. Chon, M. Shimshak, V. Srinivasan, and P. R. Guduru, J. Power Sources **195**, 5062 (2010).
[8]K. Zhao, W. L. Wang, J. Gregoire, M. Pharr, Z. Suo, J. J. Vlassak, and E. Kaxiras, Nano Lett. **11**, 2962 (2011).
[9]F. Fan, S. Huang, H. Yang, M. Raju, D. Datta, V. B. Shenoy, A. C. T. van Duin, S. Zhang, and T. Zhu, Modell. Simul. Mater. Sci. Eng. **21**, 074002 (2013).
[10]S. T. Boles, C. V. Thompson, O. Kraft, and R. Moenig, Appl. Phys. Lett. **103**, 263906 (2013).
[11]L. A. Berla, S. W. Lee, Y. Cui, and W. D. Nix, J. Power Sources **273**, 41 (2015).
[12]M. Pharr, Z. Suo, and J. J. Vlassak, J. Power Sources **270**, 569 (2014).
[13]K. Zhao, M. Pharr, Q. Wan, W. L. Wang, E. Kaxiras, J. J. Vlassak, and Z. Suo, J. Electrochem. Soc. **159**, A238 (2012).
[14]Z. Cui, F. Gao, and J. Qu, J. Mech. Phys. Solids **61**, 293 (2013).
[15]H. Yang, F. Fan, W. Liang, X. Guo, T. Zhu, and S. Zhang, J. Mech. Phys. Solids **70**, 349 (2014).
[16]H. Yang, S. Huang, X. Huang, F. Fan, W. Liang, X. H. Liu, L.-Q. Chen, J. Y. Huang, J. Li, T. Zhu, and S. Zhang, Nano Lett. **12**, 1953 (2012).
[17]A. F. Bower, P. R. Guduru, and V. A. Sethuraman, J. Mech. Phys. Solids **59**, 804 (2011).
[18]X. H. Liu, J. W. Wang, S. Huang, F. Fan, X. Huang, Y. Liu, S. Krylyuk, J. Yoo, S. A. Dayeh, A. V. Davydov, S. X. Mao, S. T. Picraux, S. Zhang, J. Li, T. Zhu, and J. Y. Huang, Nat. Nanotechnol. **7**, 749 (2012).
[19]M. T. McDowell, I. Ryu, S. W. Lee, C. Wang, W. D. Nix, and Y. Cui, Adv. Mater. **24**, 6034 (2012).
[20]S. Huang, F. Fan, J. Li, S. Zhang, and T. Zhu, Acta Mater. **61**, 4354 (2013).
[21]S. K. Soni, B. W. Sheldon, X. Xiao, A. F. Bower, and M. W. Verbrugge, J. Electrochem. Soc. **159**, A1520 (2012).
[22]Z. Zeng, N. Liu, Q. Zeng, S. W. Lee, W. L. Mao, and Y. Cui, Nano Energy **22**, 105 (2016).

Rate-dependent Stress Evolution in Nanostructured Si Anodes upon Lithiation

Supporting Online Material

Zheng Jia*, Wing Kam Liu*

Department of Mechanical Engineering, Northwestern University, IL 60201, U.S.A.

*Email: zheng.jia@northwestern.edu, w-liu@northwestern.edu

Postulated lithiation process of the interface

An approximated lithiation process of the interface is presented in Fig. S1. As shown in Fig. S1(a), at the time $t = t_0$, an interface with thickness w (~1nm) develops between the unlithiated Si phase and the fully lithiated $Li_{3.75}Si$ phase, its position is determined by the radius A of its centerline (white dashed line in the figure). Li atoms migrate into the interface and alloy with Si atoms, leading to increasing Li fraction at the interface as lithiation goes on, as illustrated in the schematics of atomic structures in Fig. S1(b) and S1(c). Eventually the interface is fully lithiated and hence merges with the fully lithiated $Li_{3.75}Si$ shell. Right after the 'old' interface is absorbed by the fully lithiated shell (at $t = t_1$), an emerging interface with the same thickness w (~1nm) emerges ahead of the 'old' one, with its position defined by a radius of $A - w$, Fig. S1(d). The whole process depicted in Fig. S1(a)-(d) occurs iteratively to evolve the lithiation of silicon anode. Note that the time needed to fill up an interface is given by $t_1 - t_0 = \frac{\beta-1}{\dot{\beta}}$, and at the meanwhile the distance travelled by the interface is w. As a result, the interface migration speed can be equivalently defined as $|\dot{A}| = w/(\frac{\beta-1}{\dot{\beta}})$; since $\beta = 4$, we have $|\dot{A}| = w/(\frac{3}{4}\frac{\beta}{\dot{\beta}})$.

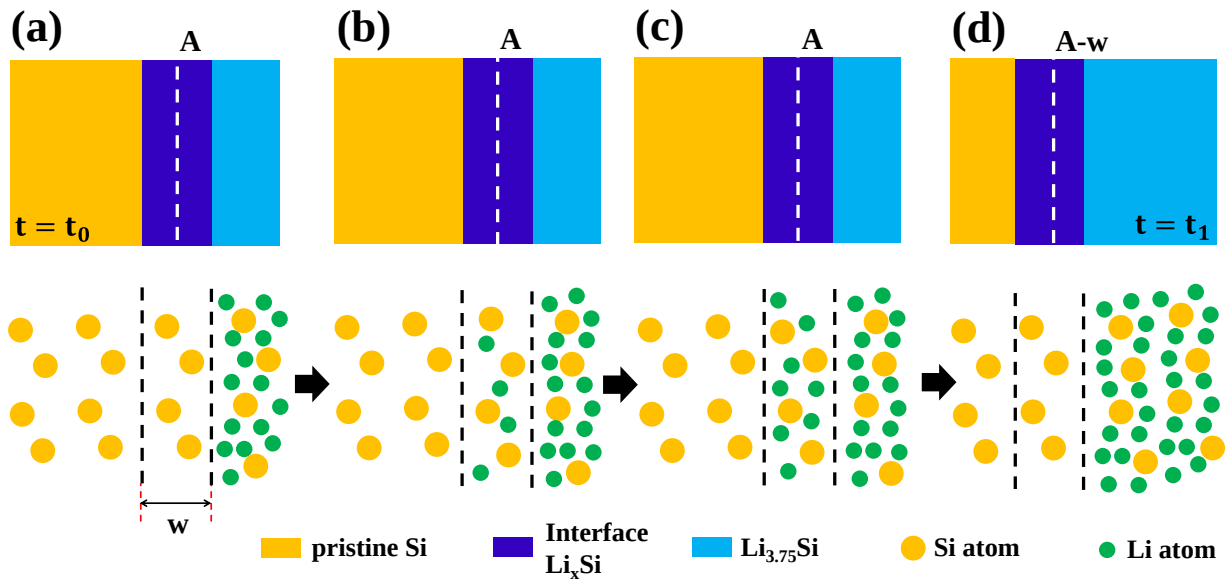

Fig. S1. Lithiation process of the Si-$Li_{3.75}Si$ interface. (a) An interface of width w (~1nm) starts to form between the unlithiated Si phase and the fully lithiated $Li_{3.75}Si$ phase. The black dashed lines delineate the interface region in the schematic of the atomic structure. (b) Li atoms migrate into the interface and react with Si atoms. The ratio of the number of Li atoms to that of Si atoms is 1. (c) Li atoms continue arriving at the interface, leading to raising Li fraction with the ratio of the number of Li atoms to that of Si atoms equal to 2. (d) Once the ratio between the number of Li atoms and that of Si atoms reaches 3.75, the 'old' interface is filled up by $Li_{3.75}Si$ phase and merges with the fully lithiated shell. An emerging interface forms ahead of the 'old' one, with a radius of $A - w$. (The schematic is just used as illustration and it does not represent the real atomic structure)